Mathematical Biology and Bioinformatics
2022. V. 17. № S. P. t42–t52. doi: 10.17537/2022.17.t42

Ttranslation of the original article.
Korshunova A.N., Lakhno V.D. Mathematical Biology and Bioinformatics. 2022;17(2):452–464. doi: 10.17537/2022.17.452

========== TRANSLATIONS OF PUBLISHED ARTICLES ==========

The Incipient Formation of the Internal Dynamics of a Uniformly Moving Polaron in a Polynucleotide Chain Subjected To a Constant Electric Field

Korshunova A.N.[*], Lakhno V.D.[**]

Institute of Mathematical Problems of Biology RAS – the Branch of Keldysh Institute of Applied Mathematics of Russian Academy of Sciences, Pushchino, Moscow Region, 142290, Russia

Abstract. In this paper, the motion of a polaron in a polynucleotide chain in an external electric field is considered. The calculations performed show that Bloch oscillations arising in the course of the polaron oscillatory motion along the chain do not completely disappear when the polaron motion along the chain becomes uniform. When the polaron moves uniformly along the chain, Bloch oscillations are also observed, although in a slightly different form. It is shown that the shape of the electron density distribution in a polaron during its stationary motion in a constant electric field takes an explicit structure. In this case, such characteristics of Bloch oscillations as the period of Bloch oscillations and the maximum Bloch amplitude demonstrate low-density components of the polaron.

Key words: *nanobioelectronics, nanowire, molecular chain, polaron, DNA, charge transfer, Holstein model.*

INTRODUCTION

In this paper we study the stationary motion of a polaron in a molecular chain in an initial period of time. The nature of Bloch oscillations of a polaron in a stationary mode is compared to that in an oscillatory mode. The polaron motion is simulated in the presence of a constant electric field on the basis of the Holstein model [1, 2]. Charge transport in DNA is considered in many theoretical works [3]–[14], which is mainly due to the possibility of using one-dimensional molecular chains as nanowires in nanobioelectronic devices [15]–[20]. Moreover, in many works, a polaron is considered to be the main current carrier in synthetic polynucleotide sequences [21]–[31].

Earlier studies show that the system under consideration can demonstrate complex dynamic regimes which depend on all the chosen parameters of the system: the frequency, the friction coefficient, the chain length, the characteristic size of the steady-state polaron in the chain, which is determined by dimensionless parameters of a bond between the electron and the lattice. It is also shown [32], that by changing only the initial charge distribution and the electric field intensity, one can observe a wide variety of modes of motion and charge distribution in a chain. The possibility for a charge occurring in a uniform Holstein chain in a constant electric field to move uniformly over very long distances is shown in [32]. Also in [32] a good agreement

[*]alya@impb.ru
[**]lak@impb.ru

was demonstrated between the theoretical [33] и and numerical dependences of the velocity of a uniform charge motion on the electric field intensity.

The uniform motion of a polaron along the chain is possible for small values of the electric field intensity. As the electric field intensity increases the charge starts oscillatory motion with Bloch oscillations. Depending on the chosen parameters of the chain, a polaron can retain its shape for some time while performing Bloch oscillations [34]. In other cases, an initial polaron can quickly disintegrate, and then the charge moves along the chain in the direction of the field, performing Bloch oscillations.

Earlier, in [35], it was shown that in the course of stationary motion along a chain in a constant electric field, a polaron executes Peierls - Nabarro oscillations due to discreteness of the chain. In this paper, it is shown that in the course of stationary motion of a polaron along a chain, a polaron demonstrates not only Peierls - Nabarro oscillations, but also small oscillations with a Bloch period.

To simulate a specific mode of charge behavior in an electric field, it is necessary to fit appropriate parameters of the system. Choosing the model parameters of the chains, we can significantly speed up and simplify the study of both the motion of a charge in the field and the nature of the charge distribution along the chain during this motion. Selection of the system parameters for each particular case is carried out not only as a result of numerical studies, but also in accordance with the results of an analytical study of the system in the continuum limit [33].

In this work, it is shown that with a uniform motion of a polaron, immediately after the instantaneous switching on of a constant electric field, the shape of the electron density distribution in the polaron takes an explicit structure. Low-density components of the polaron arise, with their own internal dynamics, different from the dynamics of the macro-part of the polaron. And, despite the fact that the polaron as a whole moves at a constant velocity, retaining its shape, the low-density components of the polaron demonstrate such characteristics of Bloch oscillations as the period of Bloch oscillations and the maximum Bloch amplitude.

MATHEMATICAL MODEL

The dynamic behavior of a polaron in the presence of a constant external field in a homogeneous molecular chain is modeled by a system of coupled quantum-classical dynamic equations with dissipation. In our model, DNA is considered as a homogeneous chain composed of N sites. Each site is a nucleotide pair, which is considered as a harmonic oscillator [31]. To simulate the dynamics of a quantum particle in a chain of N nucleotide pairs, we will use the Holstein Hamiltonian, where each site is a diatomic molecule [1, 2]:

$$\begin{aligned}\hat{H} = &-\sum_n^N \nu\Big(|n\rangle\langle n-1| + |n\rangle\langle n+1|\Big) + \sum_n^N \alpha q_n |n\rangle\langle n| \\ &+ \sum_n^N M\dot{q}_n^2/2 + \sum_n^N k q_n^2/2 + \sum_n^N e\mathcal{E}n|n\rangle\langle n|, \end{aligned} \tag{1}$$

where ν – is the matrix element of the charge transition between neighboring sites (nucleotide pairs), α – is a constant of interaction of the charge with displacements q_n, M – is the effective mass of the site, k – is the elastic constant,
e – is the electron charge, $\mathcal{E}$ – is the electric field intensity.

The equations of motion for the Hamiltonian $\hat{H}$ lead to the following system of differential equations:

$$i\hbar\dot{b}_n = -\nu(b_{n-1} + b_{n+1}) + \alpha q_n b_n + e\mathcal{E}anb_n, \tag{2}$$

$$M\ddot{q}_n = -\gamma\dot{q}_n - kq_n - \alpha|b_n|^2, \tag{3}$$

where b_n – is the amplitude of the probability of charge's occurrence on the n-th site, $\sum_n |b_n|^2 = 1$, $\hbar = h/2\pi$, h – is Planck's constant. The classical motion equations (3) involve dissipation determined by the friction coefficient γ.

Equations (2) are Schrödinger equations for the probability amplitudes b_n, which describe the evolution of a particle in a deformed chain. Equations (3) represent classical motion equations which describe the dynamics of nucleotide pairs with allowance for dissipation.

To simulate numerically the motion of a polaron, we turn to dimensionless variables using the relations:

$$\begin{aligned} \eta &= \tau\nu/\hbar\,, \quad \omega^2 = \tau^2 K/M\,, \\ \omega' &= \tau\gamma/M\,, \quad q_n = \beta u_n\,, \; E = \mathcal{E}ea\tau/\hbar, \\ \varkappa\omega^2 &= \tau^3(\alpha)^2/M\hbar\,, \; \beta = \tau^2\alpha/M\,, \quad t = \tau\tilde{t}\,, \end{aligned} \tag{4}$$

where τ – is an arbitrary time scale which relates the time t and the dimensionless variable $\tilde{t}$.

In dimensionless variables of (4) equations (2), (3) take on the form:

$$i\frac{db_n}{d\tilde{t}} = -\eta\big(b_{n+1} + b_{n-1}\big) + \varkappa\omega^2 u_n b_n + Enb_n, \tag{5}$$

$$\frac{d^2u_n}{d\tilde{t}^2} = -\omega'\frac{du_n}{d\tilde{t}} - \omega^2 u_n - |b_n|^2\,, \tag{6}$$

where b_n – are the amplitudes of the probability of charge's occurrence at the n-th site, η – are matrix elements of the transition over the sites, ω – is the frequency of oscillations of the n-th site, $\varkappa$ – is the coupling constant, ω' – is a friction coefficient, u_n – are displacements of sites from their equilibrium positions, E – is the electric field intensity, $\tilde{t} = t/\tau$, $\tau = 10^{-14}$ sec (arbitrary time scale).

The model introduced in this way is the simplest model of the dynamics of a charged particle in a polynucleotide chain, which explicitly takes into account dissipation in the system under consideration. The system of nonlinear differential equations (5), (6) is solved by fourth-order Runge–Kutta method.

In this work, we investigate the motion of polaron states in an electric field in a uniform open chain. For this study, it is essential that the chain is open and has two ends.

INITIAL DATA

In this work, to simulate the motion of a charge in an electric field, the following values of the dimensionless parameters were chosen: $\varkappa = 4$, $\eta = 2.4$.

In the absence of an external field the stationary solution of equations (5), (6) corresponds to the following function in the form of an inverse hyperbolic cosine:

$$\begin{aligned} |\,b_n(0)| &= \frac{\sqrt{2}}{4}\sqrt{\frac{\varkappa}{|\,\eta|}}\,\mathrm{ch}^{-1}\Big(\frac{\varkappa(n-n_0)}{4|\,\eta|}\Big), \\ u_n(0) &= |\,b_n(0)|^2/\omega^2, \;\; du_n(0)/d\tilde{t} = 0. \end{aligned} \tag{7}$$

Let us determine the characteristic size of the charge distribution in the chain as $\lim_{\tilde{t}\to\infty} d(\tilde{t})$, where

$$d(\tilde{t}) = \sum |b_n(\tilde{t})|^2 \Big/ \sum |b_n(\tilde{t})|^4 = 1 \Big/ \sum |b_n(\tilde{t})|^4. \tag{8}$$

The polaron corresponding to a stationary solution of equations (5), (6) in the continuum limit is not a steady polaron for a discrete chain with any given parameters. We call a steady polaron, if it does not shift from its position in the chain and does not change its shape in the

absence of an electric field or additional excitations in the chain. For large-radius polarons (for example, $d(\tilde{t}) > 15$), a polaron of the form of (7) is very close to the steady-state one, but differs significantly from narrower polarons.

For the chosen values of the parameters $\varkappa = 4$ и $\eta = 2.4$, the initial polaron state of the form of (7) differs insignificantly from the steady-state polaron for a given chain. With such parameters of the chain, the characteristic size of a polaron in the chain is $d(\tilde{t}) \approx 6.88$.

We will set the initial values of the function $|\,b_n(0)|$ in the form of a stretched inverse hyperbolic cosine:

$$|\,b_n(0)| = \frac{\sqrt{2}}{4}\sqrt{\frac{\varkappa}{\xi|\,\eta|}}\,\mathrm{ch}^{-1}\Big(\frac{\varkappa(n-n_0)}{4\xi|\,\eta|}\Big), \tag{9}$$

where ξ – is the stretching coefficient, with the help of which we can choose the initial polaron of the form of (9) as close to the steady-state polaron as possible, besides, we can take the initial polaron narrower or wider than the steady-state one for the formation of various variations of the charge motion along the chain. Thus, an expression of the form of (9), with a properly chosen value of ξ, can be considered an approximate solution to the stationary solution of equations (5), (6). For a chain with parameters $\varkappa = 4$ и $\eta = 2.4$ the inverse hyperbolic cosine or initial polaron of the form of (9) is as close as possible to the steady-state polaron for $\xi = 0.95$.

Figure 1 shows graphs of the functions $|b_n(0)|^2$ and $u_n(0)$ of the form of (9) for $\xi = 0.95$, which practically coincide with the corresponding functions of the steady polaron in a given chain, therefore it is quite possible to say that Figure 1 shows the graphs of the functions of probabilities and displacements for the steady polaron.

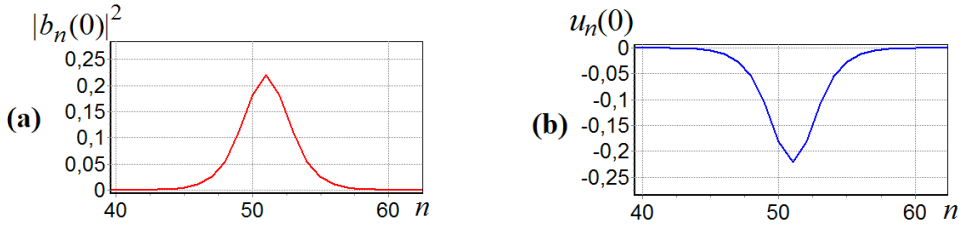

Fig. 1. Graphs of the functions $|b_n(0)|^2$ and $u_n(0)$ for the steady polaron in the center of a chain consisting of $N = 101$ sites for the values of the chain parameters $\varkappa = 4, \eta = 2.4, \omega = 1$.

Thus, to simulate the motion of a polaron in a constant electric field, we will place in the chain the initial polaron state of the form of (9) for the required values of the stretching coefficient ξ. We place the center of the polaron on the site of the chain with the number n_0. The value of n_0 is chosen so that at the beginning of the calculations the polaron be far enough from the ends of the chain. Similarly, the length of the chain is chosen so that at the end of the calculations the polaron would not come too close to the end of the chain. The field turns on ”instantly” at the initial moment of time.

BLOCH OSCILLATIONS OF A POLARON DURING AN OSCILLATORY REGIME OF MOTION

In [34] we considered in detail Bloch oscillations of a polaron in a constant electric field in a chain with parameters $\eta = 1.276, \omega = 0.1, \omega' = 0.006$ for various values of the parameter $\varkappa$. In particular, for the value $\varkappa = 1$ it is shown that the polaron in the initial period of time performs Bloch oscillations, retaining its shape, and loses its shape gradually over time. In this case, a very good agreement between the numerical and theoretical characteristics of Bloch oscillations was observed.

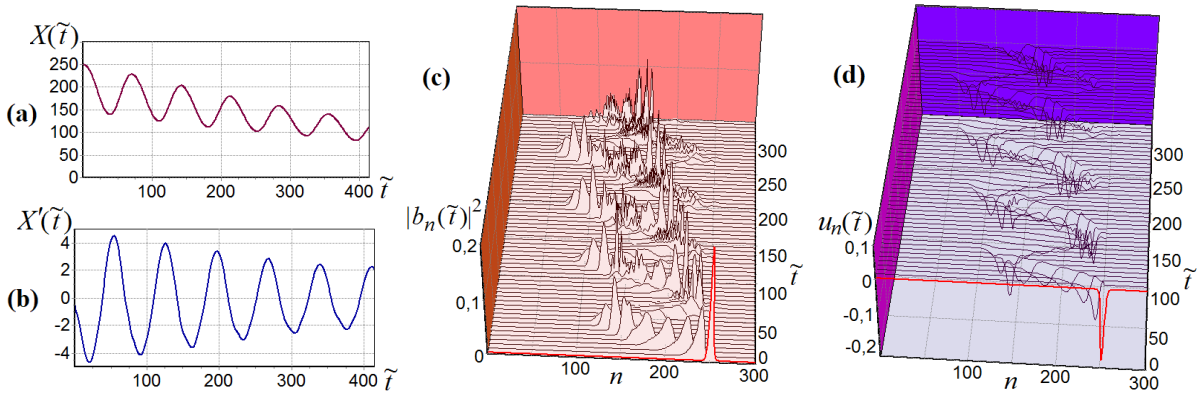

Fig. 2. Evolution of a polaron in a constant electric field of intensity $E = 0.1$ in a chain with parameters $\varkappa = 4, \eta = 2.4, \omega = 1, \omega' = 1$ and length $N = 301$ sites. The center of the polaron at the initial moment of time is located at the site of the chain with the number $n_0 = 250$. Graph (**a**) shows the function $X(\tilde{t})$, graph (**b**) shows its derivative – the function $X'(\tilde{t})$. Graph (**c**) demonstrates the dynamics of the amplitudes of the probabilities of charge localization at the nth site – the function $|b_n(\tilde{t})|^2$. Graph (**d**) shows the displacements of the chain sites during polaron motion – the function $u_n(\tilde{t})$.

The characteristics of Bloch oscillations are as follows. The period of Bloch oscillations is $T_{BL} = 2\pi/E$. The maximum Bloch amplitude is $A_{BL} = 4\eta/E$. The maximum charge rate in the process of Bloch oscillations is $V_{BL} = 2\eta$.

Figure 2 shows graphs of functions that characterize the motion and distribution of a polaron along a chain in an electric field. In the presented example, the following values of the chain parameters were selected: $\varkappa = 4, \eta = 2.4, \omega = 1, \omega' = 1$. We chose the dimensionless value of the electric field intensity $E = 0.1$ such that there is no uniform motion, the polaron immediately falls apart and starts oscillatory motion. The initial values of $|\, b_n(0)|$ were chosen in the form of an inverse hyperbolic cosine of the form of (9) for $\xi = 0.95$, that is, the initial polaron is as close as possible to the steady polaron in the chain, which is shown in Figure 1. The center of the polaron at the initial moment of time is located at the site of the chain with the number $n_0 = 250$.

Figure 2,a shows the graph of the function

$$X(\tilde{t}) = \sum\nolimits_n |\, b_n(\tilde{t})|^2 \cdot n, \tag{10}$$

which describe the motion of the center of mass of the particle. The figure 2,b shows the graph of the derivative of the function $X(\tilde{t})$ – the graph of the function $X'(\tilde{t})$. The period of Bloch oscillations for $E = 0.1$ is equal to $T_{BL} = 2\pi/E \approx 62.83$, the maximum Bloch amplitude is $A_{BL} = 4\eta/E = 96$, the maximum velocity of a charge in the process of Bloch oscillations is $V_{BL} = 2\eta = 4.8$. Thus, the graphs shown in Fig. 2 clearly demonstrate that the main characteristics of Bloch oscillations approximately correspond to theoretical characteristics. Graphs of functions $X(\tilde{t})$ and $|b_n(\tilde{t})|^2$ presented in figure 2,a and figure 2,c respectively, show that in the initial period of time the center of mass of the charge shifts by approximately the maximum Bloch amplitude, over time the amplitude of oscillations decreases, the charge continues to move along the chain in the direction of the field, performing Bloch oscillations.

The maximum charge velocity in the course of Bloch oscillations in the example considered $V_{BL} \approx 4.7$ (see Fig. 2,b) differs only slightly from the theoretical one $V_{BL} = 2\eta = 4.8$, which will not be observed when the polaron moves uniformly along the chain. Figure 2,d shows the graphs of the function $u_n(\tilde{t})$, which describes the displacements of the chain sites during the

polaron motion. Figures 2,c and 2,d clearly demonstrate that the displacements of the chain sites correspond to the probabilities of the charge distribution along the chain. Notice that such a good correspondence of the graphs of the functions $u_n(\tilde{t})$ and $|b_n(\tilde{t})|^2$ is observed for large values of the parameters $\omega = 1$ and $\omega' = 1$. For small values of ω and ω' such a good correspondence of these plots is not observed.

ELEMENTS OF BLOCH POLARON OSCILLATIONS IN THE COURSE OF ITS UNIFORM MOTION ALONG A CHAIN IN A CONSTANT ELECTRIC FIELD

In this section, we will show that elements of Bloch oscillations also appear in the case of a stationary motion of a polaron along a chain. To simulate the uniform motion of a charge in a constant electric field, the following values of the dimensionless parameters were chosen: $\varkappa = 4, \eta = 2.4, \omega = 1, \omega' = 1$.

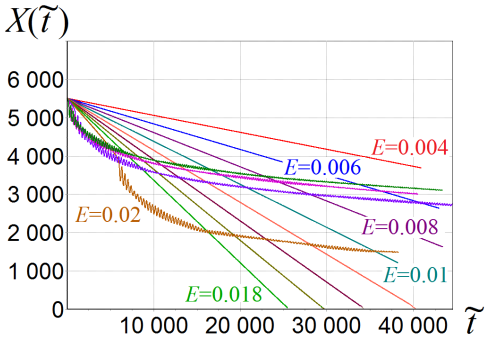

Fig. 3. Polaron motion in a constant electric field for different values of the field intensity. The graphs of the function $X(\tilde{t})$ are presented for $E = 0.004$ (top graph), $0.006, ...0.026$. Uniform polaron motion of are observed for $E = 0.004$, ... 0.018. The values of the chain parameters are $\varkappa = 4$, $\eta = 2.4$, $\omega = 1$, $\omega' = 1$. The center of the polaron at the initial moment of time is at the site of the chain with the number $n_0 = 5500$. The chain length is $N = 7001$ sites.

The graphs of the function $X(\tilde{t})$ shown in Figure 3 demonstrate a linear dependence on $\tilde{t}$ for the values of the electric field intensity $E = 0.004, E = 0.006, ...E = 0.018$. The maximum computation time for the graphs shown exceeds the dimensionless time $\tilde{t} = 40000$. For each graph of the function $X(\tilde{t})$ in Figure 3 the duration of calculations exceeds tens of Bloch periods corresponding to a given electric field intensity. This undoubtedly suggests that for the indicated values of the electric field intensity, we observe a uniform motion of a polaron along the chain, at least on the time intervals shown.

Let us consider in greater detail the distribution of the initial polaron along the chain during its uniform motion in an electric field of intensity $E = 0.018$. Figure 3 shows that for the chosen value of the electric field intensity, the duration of the uniform motion is $\tilde{t} > 25000$.

Figure 4 shows the graphs of the functions $X(\tilde{t}), X'(\tilde{t}), |b_n(\tilde{t})|^2$, which characterize the motion and distribution of a polaron along a chain in an electric field of intensity $E = 0.018$. The initial values of $|b_n(0)|$ were chosen in the form of an inverse hyperbolic cosine as (9) for $\xi = 0.95$. Such a polaron is as close as possible to the steady polaron in the chain. The chain length is $N = 1101$ sites. The center of the polaron at the initial moment of time is located at the site of the chain with the number $n_0 = 900$. For the chosen value of the electric field intensity $E = 0.018$ the period of Bloch oscillations is $T_{BL} = 2\pi/E \approx 349$. The maximum Bloch amplitude is $A_{BL} = 4\eta/E \approx 533$. The graphs shown in Figure 4 demonstrate that the main characteristics of Bloch oscillations are approximately observed. The graph of the function $X'(\tilde{t})$ in Figure 4,b demonstrates the period of Bloch oscillations, approximately equal to the theoretical period: $T_{BL} \approx 349$. The oscillation amplitude of the function $X'(\tilde{t})$ is very small.

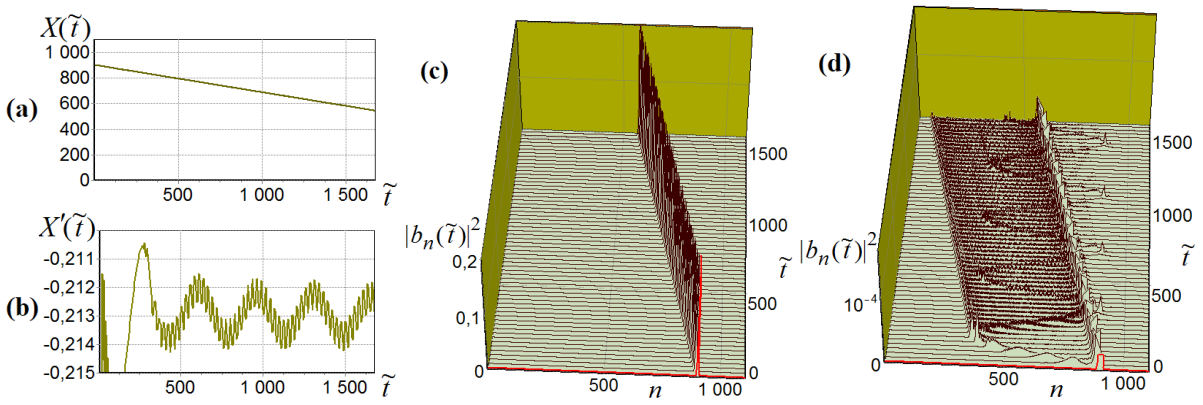

Fig. 4. Uniform motion of a polaron in a constant electric field of intensity $E = 0.018$. Graphs of the functions $X(\tilde{t}), X'(\tilde{t}), |b_n(\tilde{t})|^2$ during the motion of a polaron in a chain with parameters $\varkappa = 4, \eta = 2.4, \omega = 1, \omega' = 1$ and length $N = 1101$ sites. The center of the polaron at the initial moment of time is located at the site of the chain with the number $n_0 = 900$.

And yet, the graphs of the functions $X(\tilde{t})$ in Figure 4,a and $|b_n(\tilde{t})|^2$ in Figure 4,c indicate the uniform motion of the polaron along the chain. The oscillation amplitude of the function $X'(\tilde{t})$ is very small, its values vary from $X'(\tilde{t}) \approx -0.212$ to $X'(\tilde{t}) \approx -0.214$. The view of smaller oscillations $X'(\tilde{t})$ in Figure 4,b is due to the discreteness of the output of the function on the graph and, mainly, the proximity of the location of the charge to the end of the chain. When these conditions for plotting the graph of the function $X'(\tilde{t})$ change, only the form of the smallest oscillations changes. For example, when the values of $X'(\tilde{t})$ are displayed more frequently, the small oscillations merge (at the scale of the graph in Fig. 4,b) and the graph $X'(\tilde{t})$ looks like a solid line. At the same time, the larger oscillations with the Bloch period fully correspond to the oscillations in Figure 4,b.

Figure 4,d shows the same graph of the function $|b_n(\tilde{t})|^2$, as in Figure 4,c, but on a different scale. The mark on the left-hand scale indicates a value of 10^{-4}. Besides, only those values of the function $|b_n(\tilde{t})|^2$, which are less than $5 \cdot 10^{-5}$, are displayed on the graph. The values of $|b_n(\tilde{t})|^2 > 5 \cdot 10^{-5}$ in Figure 4,d are as if truncated so that the low-density components of the function $|b_n(\tilde{t})|^2$ be visible.

The graph of the function $|b_n(\tilde{t})|^2$ in Figure 4,d shows that, in the very initial period of time, approximately equal to half the Bloch period, during the dimensionless time $\tilde{t} \approx 175 \approx 349/2$, the low-density part of the polaron is pushed out in front of the polaron itself in the direction of the polaron motion over the sites by the width approximately equal to the maximum Bloch amplitude $A_{BL} \approx 533$. During the second half of the Bloch period from the beginning of the motion, this part that emerged in front of the polaron returns to the initial position in the center of the polaron. During this first Bloch period, the center of the polaron travelled several sites, and since we cut off most of the polaron, we can see that the excitation that came out in front of the polaron passed back through the main part of the polaron exactly to the initial position of the center of the polaron. Notice that when the charge moves oscillatorily along the chain, in the initial period of time, the charge is also displaced by approximately the maximum Bloch amplitude, but in this case the center of mass of the charge is also displaced by approximately the same value, see Figure 2. With further motion of the polaron along the chain the initial excitation oscillates with a Bloch period, being at the chain sites located from the center of the initial polaron to the side in the direction of the field by the width of approximately one maximum Bloch amplitude.

Figure 4,d clearly demonstrates how a low-density polaron component emerges in front of the polaron in the first half of the first Bloch period. But during the second half of the first

Bloch period, only part of the excitation comes back. That is, in the second half of the first Bloch period, we already observe two low-density components of the polaron. One of them is oscillating low-density component. The other excitation moves in front of the polaron, with the velocity of the polaron, has a constant distribution width over the sites which is approximately equal to the maximum Bloch amplitude for a given value of the electric field. No oscillations are observed in the second low-density component. We have called this low-density component precursor component. Obviously, the precursor low-density component is formed due to the presence of a polaron in the chain, which retains its shape.

Graphs of the functions $u_n(\tilde{t})$ in Figure 5 illustrate displacements of the sites of the chain in the same computational experiment which is shown in Figure 4. In Figure 5,a the graphs of the functions $u_n(\tilde{t})$ are shown full-scale. In Figure 5,b, by analogy with Figure 4,d, truncated graphs of the functions $u_n(\tilde{t})$ are shown. The bottom mark on the left scale is equal -10^{-4}.

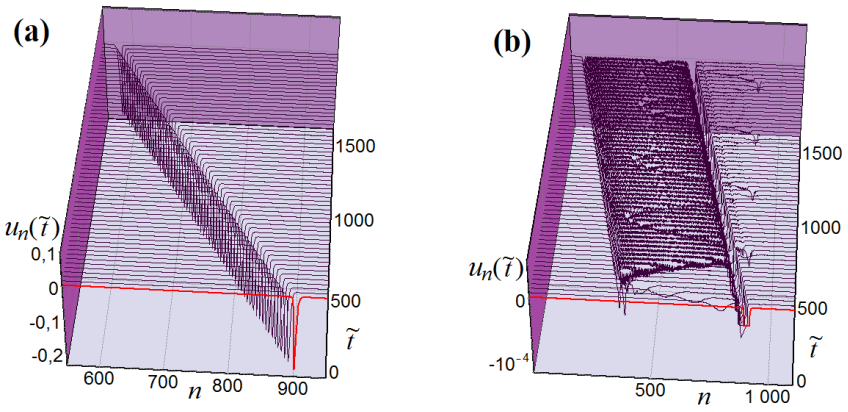

Fig. 5. Graphs of the functions $u_n(\tilde{t})$ in the course of a uniform motion of a polaron in a chain with the parameters $\varkappa = 4, \eta = 2.4, \omega = 1, \omega' = 1$ and the length of $N = 1101\ 1101$ sites. The center of the polaron at the initial moment of time is at the site of the chain with the number $n_0 = 900$. The electric field intensity is $E = 0.018$.

From the presented in Figure 5 graphs of the functions $u_n(\tilde{t})$ follows, that the site displacements correspond to the probability distribution functions $|b_n(\tilde{t})|^2$ shown in Figure 4. Such a good correspondence between the site displacements $u_n(\tilde{t})$ and the probability distribution functions $|b_n(\tilde{t})|^2$ is observed for large values of the oscillation frequency of the chain sites $\omega = 1$ and a large value of the friction coefficient $\omega' = 1$. For small values of these parameters, for example, for $\omega = 0.01$ $\omega' = 0.006$, which correspond to the parameters of the DNA chain, the forms of the graphs of the functions $u_n(\tilde{t})$ and $|b_n(\tilde{t})|^2$ are slightly different from each other. Thus, in the case of a uniform motion of a polaron along the chain, the low-density components of the polaron form displacements of the chain sites, the shape of which depends on the chain parameters.

CONCLUSION

The calculations performed showed that the elements of Bloch oscillations are also observed in the case of stationary motion of a polaron along a chain. It is shown that for stationary motion of a polaron along a chain in a constant electric field, the graphs of the functions $X(\tilde{t})$, which describe the position of the center of mass of the polaron, demonstrate a linear dependence on $\tilde{t}$ for sufficiently large values of the parameters ω and ω', for example, for $\omega = 1, \omega' = 1$. In this case, the derivative of the function $X(\tilde{t})$ performs very insignificant amplitude oscillations with a Bloch period. For small values of the parameters ω и ω', for example, for $\omega = 0.01, \omega' = 0.006$,

low-amplitude oscillations with a Bloch period are noticeable on the graph of the function $X(\tilde{t})$, while the polaron maximum moves strictly in the direction of the field, without performing oscillations, in the same way as for large values of the parameters ω and ω'.

It is shown that in the case of a uniform motion of a polaron along a chain in the initial period of time, two low-density components of the polaron are formed: oscillating low-density component, which retains its position in the chain, and the precursor low-density component moving in front of the polaron per se.

The oscillating low-density component of the polaron is located between the site at which the center of the initial polaron have placed and the site that is spaced from the initial position by the value of the maximum Bloch amplitude in the direction of the field. The width of the oscillating low-density component distribution over the sites is approximately equal to one maximum Bloch amplitude. At the initial instant of time, the width of the oscillating low-density component can slightly increase with a change in the shape of the initial polaron state or with a decrease in the parameters ω and ω'. When the values of the parameters ω and ω' decrease, the values of the functions $|b_n(\tilde{t})|^2$, related to the oscillating low-density component, increase. Over time, oscillating low-density component of the polaron spreads out a little, but retains its position in the chain within approximately one maximum Bloch amplitude. From the very beginning of the motion, this low-density polaron component performs oscillations, the period of which is close to the period of Bloch oscillations for a given electric field intensity.

The precursor low-density component also depends on the values of the parameters ω and ω'. The values of the functions $|b_n(\tilde{t})|^2$, corresponding to the precursor component depend in direct proportion on the values of the friction coefficient: the smaller is the value of the friction coefficient, the smaller is the values of the functions $|b_n(\tilde{t})|^2$ in the precursor component.

Modeling of a uniform motion of a polaron along a chain for different values of the electric field intensity demonstrates that the width of the distribution over the sites of the low-density components of the polaron - the oscillating and the precursing one - is approximately equal to one maximum Bloch amplitude corresponding to a given value of the electric field intensity. Period of the oscillating low-density component of the polaron is preserved during the entire time of modeling the uniform motion of the polaron and is approximately equal to the period of Bloch oscillations for a given value of the electric field intensity.

In this work, we have considered the incipient formation of low-density components of the polaron in the initial period of motion. Longer calculations show that the macropart of the polaron passes through the region where the oscillating component of the polaron is located and moves further along the chain in the direction of the field together with the precursing component. Between the polaron macropart and the oscillating component remaining in place, we observe a region of nonzero values of the electron density distribution, these values are also very small. Thus, the macropart of the polaron, together with the precursor low-density component, are move away from the oscillating component of the polaron. The duration of this phase of motion depends on the electric field intensity, the greater the value of the electric field intensity, the shorter the duration of this motion. Then the polaron, namely, its macro part, begins to slowly collapse and, having lost its shape, passes into an oscillatory mode of motion with Bloch oscillations. In the course of the oscillatory mode of charge motion, the low-density components of the polaron, of course, are not observed, since there is no polaron itself.

ACKNOWLEDGMENTS

This study was performed using the computing resources of The Joint Supercomputer Center of the Russian Academy of Sciences (JSCC RAS).

REFERENCES

1. Holstein T. Studies of polaron motion: Part I. The molecular-crystal model. *Annals of Phys.* 1959. V. 8. P. 325–342. doi: 10.1016/0003-4916(59)90002-8
2. Holstein T. Studies of polaron motion: Part II. The ”small” polaron. *Annals of Phys.* 1959. V. 8. P. 343–389. doi: 10.1016/0003-4916(59)90003-X
3. Hennig D., Starikov E.B., Archilla J.F.R., Palmero F. Charge Transport in Poly(dG)–Poly(dC) and Poly(dA)–Poly(dT) DNA Polymers. *Journal of Biological Physics.* 2004. V. 30. №3. P. 227–238. doi: 10.1023/B:JOBP.0000046721.92623.a9
4. Huang Z., Hoshina M., Ishihara H., Zhao Y. Transient dynamics of super Bloch oscillations of a one dimensional Holstein polaron under the influence of an external AC electric field. *Annalen der Physik.* 2017. V. 529. P. 1600367. doi: 10.1002/andp.201600367
5. Hennig D., Burbanks A.D., Osbaldestin A.H. Directed current in the Holstein system. *Phys. Rev. E.* 2011. V. 83. P. 031121. doi: 10.1103/PhysRevE.83.031121
6. Yakushevich L.V., Balashova V.N., Zakiryanov F.K. On the DNA Kink Motion Under the Action of Constant Torque. *Math. Biol. Bioinf.* 2016. V. 11. №1. P. 81–90. doi: 10.17537/2016.11.81
7. Starikov E.B., Lewis J.P., Sankey O.F. Base sequence effects on charge carrier generation in DNA: a theoretical study. *International Journal of Modern Physics B.* 2005. V. 19. №29. P. 4331–4357. doi: 10.1142/S0217979205032802
8. Davydov A.S. *Solitons in Molecular systems*. Boston, USA: Reidel Publ. Comp., 1985. 413 p.
9. Scott A.C. Davydov’s soliton. *Phys. Rep.* 1992. V. 217. №1. P. 1–67. doi: 10.1016/0370-1573(92)90093-F
10. De Pablo P.J., Moreno-Herrero F., Colchero J., Gómez Herrero J., Herrero P., Baró A.M., Ordejón P., Soler J.M., Artacho E. Absence of dc-Conductivity in λ–DNA. *Phys. Rev. Lett.* 2000. V. 85. P. 4992–4995. doi: 10.1103/PhysRevLett.85.4992
11. Porath D., Bezryadin A., De Vries S., Dekker C. Direct measurement of electrical transport through DNA molecules. *Nature.* 2000. V. 403. P. 635–638. doi: 10.1038/35001029
12. Yoo K.-H., Ha D.H., Lee J.-O., Park J. W., Kim Jinhee, Kim J.J., Lee H.-Y., Kawai T., Choi Han Yong. Electrical Conduction through Poly(dA)–Poly(dT) and Poly(dG)–Poly(dC) DNA Molecules. *Phys. Rev. Lett.* 2001. V. 87. P. 198102. doi: 10.1103/PhysRevLett.87.198102
13. Kasumov A.Y., Kociak M., Guéron S., Reulet B., Volkov V.T., Klinov D.V., Bouchiat H. Proximity-Induced Superconductivity in DNA. *Science.* 2001. V. 291. № 5502. P. 280–282. doi: 10.1126/science.291.5502.280
14. Chepeliaskii A., Klinov D., Kasumov A., Guéron S., Pietrement O., Lyonnais S., Bouchiat H. Conduction of DNA molecules attached to a disconnected array of metallic Ga nanoparticles. *New J. Phys.* 2011. V. 13. P. 063046. doi: 10.1088/1367-2630/13/6/063046
15. Porath D., Cuniberti G., Di Felice R. Charge transport in DNA-based devices. *Top. Curr. Chem.* 2004. V. 237. P. 183–227. doi: 10.1007/b94477
16. Chetverikov A.P., Ebeling W., Lakhno V.D., Velarde M.G. Discrete-breather-assisted charge transport along DNA-like molecular wires. *Phys. Rev. E.* 2019. V. 100. P. 052203. doi: 10.1103/PhysRevE.100.052203
17. Eudres R.G., Cox D.L., Singh R.R.P. Colloquium: The quest for high-conductance DNA. *Rev. Mod. Phys.* 2004. V. 76. P. 195–214. doi: 10.1103/RevModPhys.76.195
18. Lakhno V.D. DNA nanobioelectronics. *Int. Quantum. Chem.* 2008. V. 108. P. 1970–1981. doi: 10.1002/qua.21717
19. *Nanobioelectronics - for Electronics, Biology and Medicine*. Eds. Offenhausser A., Rinald R. N. Y.: Springer. 2009.

20. Taniguchi M., Kawai T. DNA electronics. *Physica E.* 2006. V. 33. P. 1–12. doi: 10.1016/j.physe.2006.01.005
21. Conwell E.M., Rakhmanova S.V. Polarons in DNA. *Proc. Natl. Acad. Sci.* 2000. V. 97. P. 4556–4560. doi: 10.1073/pnas.050074497
22. Voulgarakis Nikolaos K. The effect of thermal fluctuations on Holstein polaron dynamics in electric Field. *Physica B.* 2017. V. 519. P. 5–20. doi: 10.1016/j.physb.2017.04.030
23. Fialko N.S., Lakhno V.D. Dynamics of Large Radius Polaron in a Model Polynucleotide Chain with Random Perturbations. *Math. Biol. Bioinf.* 2019. V. 14. №2. P. 406–419. doi: 10.17537/2019.14.406
24. Fuentes M.A., Maniadis P., Kalosakas G., Rasmussen K.Ø. Bishop A.R., Kenkre V.M., Gaididei Yu.B. Multipeaked polarons in soft potentials. *Phys. Rev. E.* 2004. V. 70. P. 025601(R). doi: 10.1103/PhysRevE.70.025601
25. Maniadis P., Kalosakas G., Rasmussen K.Ø., Bishop A.R. Polaron normal modes in the Peyrard-Bishop-Holstein model. *Phys. Rev. B.* 2003. V. 68. P. 174304. doi: 10.1103/PhysRevB.68.174304
26. Astakhova T.Yu., Vinogradov G.A. Polaron in Electric Field and Vibrational Spectrum of Polyacetylene. *Mathematical Biology and Bioinformatics.* 2019. V. 14. № 1. P. 150–159. doi: 10.17537/2019.14.150
27. Voityuk A.A., Rösch N., Bixon M., Jortner J. Electronic Coupling for Charge Transfer and Transport in DNA. *J. Phys. Chem. B.* 2000. V. 104. № 41. P. 9740–9745. doi: 10.1021/jp001109w
28. Jortner J., Bixon M., Voityuk A.A., Rösch N.J. Superexchange Mediated Charge Hopping in DNA. *Phys. Chem. A.* 2002. V. 106. P. 7599–7606. hdoi: 10.1021/jp014232b
29. Lakhno V.D., Korshunova A.N. Formation of stationary electronic states in finite homogeneous molecular chains. *Mathematical Biology and Bioinformatics.* 2010. V. 5. №1. P. 1–29. doi: 10.17537/2010.5.1
30. Korshunova A.N., Lakhno V.D. A new type of localized fast moving electronic excitations in molecular chains. *Physica E.* 2014. V. 60. P. 206–209. doi: 10.1016/j.physe.2014.02.025
31. Lakhno V.D. Soliton-like Solutions and Electron Transfer in DNA. *J. Biol. Phys.* 2000. V. 26. P. 133–147. doi: 10.1023/A:1005275211233
32. Korshunova A.N., Lakhno V.D. Simulation of the Stationary and Nonstationary Charge Transfer Conditions in a Uniform Holstein Chain Placed in Constant Electric Field. *Technical Physics.* 2018. V. 63. №9. P. 1270–1276. doi: 10.1134/S1063784218090086
33. Lakhno V.D. Davydov's solitons in a homogeneous nucleotide chain. *Int. J. Quant. Chem.* 2010. V. 110. P. 127–137. doi: 10.1002/qua.22264
34. Lakhno V.D., Korshunova A.N. Bloch oscillations of a soliton in a molecular chain. *Eur. Phys. J. B.* 2007. V. 55. P. 85–87. doi: 10.1140/epjb/e2007-00045-3
35. Lakhno V.D., Korshunova A.N. Electron motion in a Holstein molecular chain in an electric field. *Euro. Phys. J. B.* 2011. V. 79. P. 147–151. doi: 10.1140/epjb/e2010-10565-2

Accepted 17.12.2022.
Published 27.12.2022.